

Fission-Imposed Limits to the Angular Momentum Carried by Evaporation Residues from the Compound Nucleus ^{200}Pb

J. R. Leigh, D. J. Hinde, J. O. Newton, W. Galster, and S. H. Sie^(a)

*Department of Nuclear Physics, Research School of Physical Sciences,
Australian National University, A.C.T. 2600, Australia*

(Received 1 December 1981)

Two reactions, $^{181}\text{Ta} + ^{19}\text{F}$ and $^{170}\text{Er} + ^{30}\text{Si}$, have been used to produce ^{200}Pb . Measurements of fission and evaporation residues allow the fission probability to be obtained as a function of input angular momentum. Fission sets a sharp limit ($\sim 35\hbar$) to the angular momentum which can be observed in the evaporation residues.

PACS numbers: 25.70.Fg, 25.70.Bc, 25.85.Ge

At high angular momenta and excitation energies nuclei can decay by emission of neutrons, charged particles, or fission. Where neutron evaporation dominates, (heavy ion, xn) reactions lead to high-spin γ -ray emitting states. The study of these γ rays has so far been a prolific source of nuclear structure information at high spin.¹ The nucleus has a larger deformation and hence larger moment of inertia at the saddle point than at the equilibrium deformation. Thus the fission barrier, which is the difference in energy of these two rotating shapes, decreases with increasing angular momentum. Fission may therefore set an upper limit to the angular momentum for which nuclear structure can be studied by γ -ray techniques. Previous measurements of the competition between neutron emission and fission²⁻⁴ have not been made with sufficient detail or accuracy to indicate where this limit lies.

Here we report on a study of fission and evaporation residue (ER) excitation functions following the reactions $^{181}\text{Ta} + ^{19}\text{F}$ and $^{170}\text{Er} + ^{30}\text{Si}$ leading to the compound nucleus ^{200}Pb . The angular momentum dependence of the total fission probability has been extracted from our data.

Beams of ^{19}F (80–126 MeV) and ^{30}Si (125–168 MeV) from the Australian National University 14UD pelletron were used to bombard targets ranging in thickness from $750 \mu\text{g}/\text{cm}^2$ (self supporting) to $40 \mu\text{g}/\text{cm}^2$ (on C backings). Excitation functions and angular distributions for fission fragments and ER's were measured. Fission fragments were identified with use of a gas ionization chamber for energy-loss measurement in conjunction with silicon surface-barrier detectors. The time of flight of the ER's clearly distinguished them from other products with the same energy. Individual ER channels were identified by measuring excitation functions for (HI, $xn\gamma$) reactions with use of standard γ -ray techniques. Full experimental details will be pub-

lished.⁵

The cross sections for fission (σ_f) and for ER's (σ_{ER}) were combined to give those for complete fusion (σ_{CN}). Values of σ_{CN} plotted against the inverse center-of-mass energy $E_{\text{c.m.}}$ are shown in Fig. 1(a). The data generally follow the relationship $\sigma_{\text{CN}} = \pi R_B^2 (1 - V_B/E_{\text{c.m.}})$ except at the lowest bombarding energies where barrier penetration and deformation effects may be important⁶; here V_B is the height of the fusion barrier and R_B is its radius. In Fig. 1(b) the total fission probability, $P_f = \sigma_f/\sigma_{\text{CN}}$, is plotted against the excitation energy (E_x) in the compound system; E_x is measured relative to the ground state of a "liquid-drop nucleus" rather than that of the real ground state of ^{200}Pb , from which it differs by ~ 7 MeV. This procedure is used since ^{200}Pb is produced at high energy and angular momentum where shell and pairing effects are expected to be weak,⁷ and thus the liquid-drop mass seems most appropriate. Support for this approach comes from the (HI, $xn\gamma$) excitation functions which are well fitted by statistical-model calculations⁸ only when liquid-drop masses and binding energies are used.

When the compound nucleus is produced at the same value of E_x [Fig. 1(b)], the P_f for the ^{30}Si -induced reaction is considerably higher than that for ^{19}F . This enhancement is due to the higher orbital angular momentum ($L\hbar$) brought in by ^{30}Si . The fission probability associated with this additional angular momentum was evaluated as follows.

The angular momentum distributions in the compound system were obtained from the expression $\sigma_{\text{CN}} = \pi\lambda^2 \sum_L (2L+1)T_L$, where λ is the asymptotic reduced wave length. The transmission coefficients, T_L , were evaluated by varying the parameters of the parabolic-barrier approximation used in the statistical-model code MBII⁸ to fit the σ_{CN} data [Fig. 1(a)]; the empirical method of Vaz and Alexander⁹ was used to take deforma-

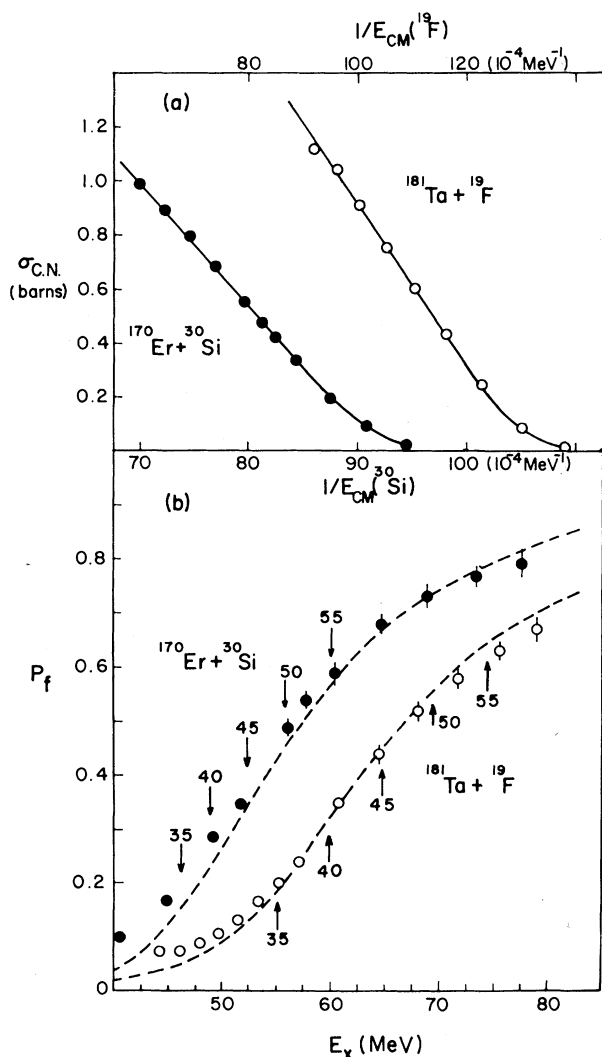


FIG. 1. (a) Measured fusion excitation functions. The curves are fits to the data using the parabolic-barrier approximation (see text). (b) Experimental total fission probabilities. The curves are MBH calculations with $a_f/a_n = 1$ and $B_f = 0.83$. The relatively poor fit at bombarding energies near the Coulomb barrier arises from the sensitivity of the calculation to the input angular momentum distribution, and the possibility of shell and pairing effects becoming important for low L and E_x . The vertical arrows indicate L_{max} , for each reaction.

tion effects into account. Thus the angular momentum distributions $\sigma_L^* = (2L + 1)T_L$ for the two reactions at each excitation energy were obtained. These are illustrated in Fig. 2(a) for $E_x = 59$ MeV; the additional angular momentum associated with the ^{30}Si reaction is shown by the difference between these distributions. It has a centroid $\bar{L} \sim 45\hbar$ and a width (full width at half maximum) of about $18\hbar$. While \bar{L} varies rapidly with E_x , the

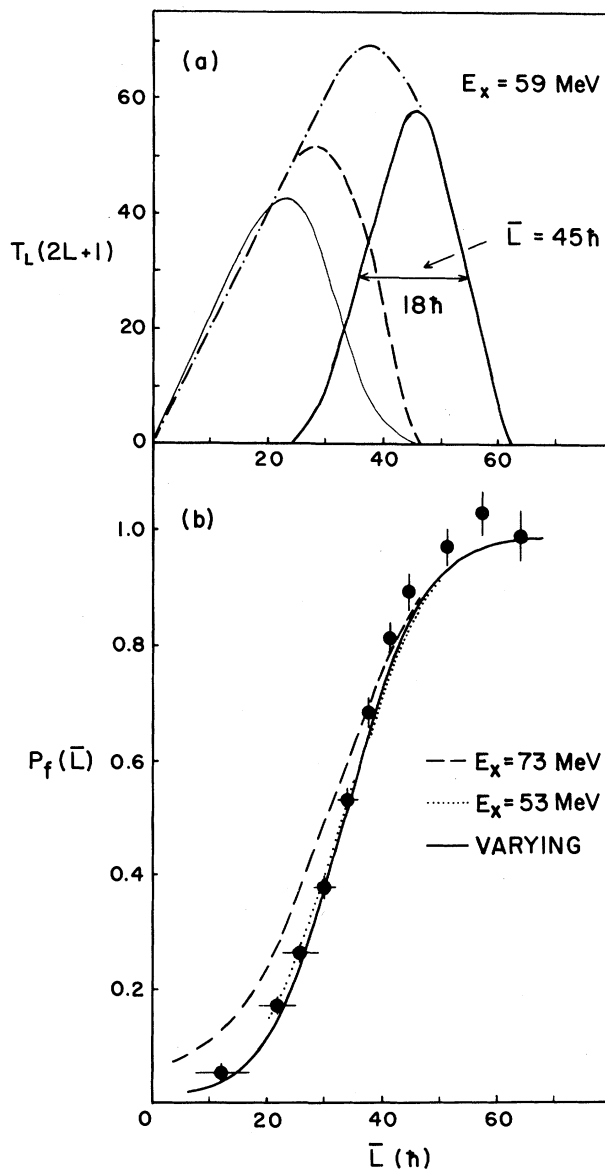


FIG. 2. (a) Calculated angular momentum distributions for forming ^{200}Pb with $^{170}\text{Er} + ^{30}\text{Si}$ (dot-dashed curve) and $^{181}\text{Ta} + ^{19}\text{F}$ (dashed curve). The full curve shows the additional angular momentum brought in by the heavier projectile. The full fine curve is the angular momentum distribution of evaporation residues following the ^{30}Si reaction. (b) MBH calculations of the total fission probabilities compared with the experimental data. The full curve is for E_x varying in the same manner as the data, while the others are for fixed E_x .

width is roughly constant. Following Zebelman *et al.*,⁴ assuming the Bohr independence hypothesis, and defining the reduced cross section $\sigma_{CN}^* = \sigma_{CN} / \pi\lambda^2$, we have the total fission probability

for the difference distribution,

$$P_f(\bar{L}) = (P_f \sigma_{CN}^* - P_f' \sigma_{CN}^{*'}) / (\sigma_{CN}^* - \sigma_{CN}^{*'}); \quad (1)$$

the primed values are those for ^{19}F bombardment and the others for ^{30}Si . Since the experimental values of P_f and P_f' were not in fact measured at identical values of E_x , one of the values has to be obtained by interpolation. This procedure is likely to involve little error as can be seen in Fig. 1(b). Values of $P_f(\bar{L})$, plotted in Fig. 2(b), were calculated from Eq. (1) at a series of excitation energies, and hence different mean angular momenta \bar{L} . The horizontal error bars are estimated by taking half the difference between the calculated \bar{L} and that from the extreme sharp cut-off model. Thus it is clear that these results depend only weakly on the estimated T_L distributions.

Each datum point corresponds to a different E_x , a total range of about 32 MeV being covered in Fig. 2(b). The first indication that the variation with E_x is not very important appears in Fig. 1(b). The calculated maximum angular momenta L_{\max} , where σ_L^* drops to half its maximum value, are shown for the two reactions. It is evident that these values of L_{\max} differ only marginally ($\lesssim 2\hbar$) for identical P_f . That is, for the same distribution, the P_f values are very nearly equal even though the values of E_x differ by as much as 15 MeV.

This insensitivity of $P_f(\bar{L})$ to E_x arises partly because the appropriate excitation energy is not E_x but rather $U_x = E_x - E_{\text{rot}}$, where E_{rot} is the rotational energy associated with the equilibrium deformation. The complete range of U_x is then only about 13 MeV. Also the range of U_x over which $P_f(\bar{L})$ varies rapidly, say from 0.2 to 0.8, is only about 6 MeV. Thus we would expect Fig. 2(b) to give a good representation of $P_f(\bar{L})$ for ^{200}Pb at an average U_x of about 50 MeV.

The P_f vs E_x data have been fitted with use of MBI [Fig. 1(b)]. The fission barrier was assumed to be given by $E_f(L) = B_f E_f^{\text{RLD}}(L)$, where E_f^{RLD} is the barrier given by the rotating liquid-drop model (RLDM),¹⁰ and B_f is a scaling factor independent of L . The only free parameters were taken to be B_f and a_f/a_n ; a_f and a_n are the level density parameters at the saddle point and at equilibrium deformation after neutron decay, respectively. The value $a_n = A/10$ was used. The results were fitted by parameter sets having a_f/a_n between 1.04 and 0.85 with B_f correspondingly between 0.86 and 0.69. The excellent quality of the fits suggests that the variation of $E_f(L)$ with

L and with A is given rather well by the RLDM. This conclusion is supported by systematic studies of the light Pb isotopes down to the compound nucleus ^{192}Pb .⁵ While one should be cautious in expecting the parameter a_f/a_n to have the theoretically expected value, because of considerable oversimplification in the statistical-model calculations, a value $a_f/a_n = 1$ gives $B_f = 0.83$, in agreement with other recent results.³ The curves of $P_f(\bar{L})$ vs \bar{L} shown in Fig. 2(b) were obtained by treating the MBI calculations in the same way as the data. This has been done for values of E_x varying in the same manner as the data, and also for fixed values of E_x . These curves are very similar for $P_f(\bar{L}) \gtrsim 0.3$ and support the observation made earlier that $P_f(\bar{L})$ is almost independent of E_x in this mass region.

The limiting L for (HI, xn) reactions, related to the steeply rising part of the $P_f(\bar{L})$ vs \bar{L} curve, is also likely to be fairly independent of U_x for other cases, though not having the same value. The reason for this can be seen from the simple formula¹¹ for the ratio of fission and neutron decay widths,

$$\Gamma_f(L)/\Gamma_n = 5(TA^{2/3})^{-1} \exp\{[B_n - E_f(L)]/T\}, \quad (2)$$

where T is the nuclear temperature when the level density is assumed to be proportional to $\exp(U_x/T)$, A is the mass number, and B_n is the neutron binding energy. For normal values of T of the order of unity ($T \propto U_x^{1/2}$), this expression achieves a value of about 15% when $E_f = B_n$ and rises rapidly as $E_f(L)$ falls below B_n with increasing L . For values of $B_n - E_f \approx 0$, Γ_f/Γ_n depends very weakly on U_x . The quantity P_f is not $\Gamma_f/(\Gamma_f + \Gamma_n)$, the fission probability for the decay of the compound system (assuming that fission and neutron emission are the only significant modes of decay). Rather it involves fission decay in competition with all steps of the neutron cascade. Assuming that Γ_f/Γ_n has a constant value of 15%, for a typical cascade of five steps we find $P_f \approx 0.5$. Thus in this simple approximation the region where Γ_f/Γ_n is approximately independent of U_x comes around $P_f = 0.5$, the most steeply rising part of the P_f vs L curve. The real situation is of course more complex than this but it still seems likely that the simple result above holds fairly well, as shown in Fig. 2(b).

The angular momentum distribution of the ER's from ^{200}Pb ($E_x = 59$ MeV) produced in the ^{30}Si reaction is shown in Fig. 2(a). The population of states with spin $> 35\hbar$ is only 1.5% of the fusion cross section and with present γ -ray techniques

it is unlikely that the effect of this small population could be observed.

From our data we have shown how $P_f(\bar{L})$ varies with L for ^{200}Pb and how the (HI, xn) cross sections are limited by fission. For ^{200}Pb the maximum angular momentum for which γ -ray studies can be performed is $\sim 35\hbar$. This fission limit rises rapidly for lighter compound systems for which other limits, due, e.g., to incomplete fusion,¹² may be relevant. Statistical-code calculations have indicated that $E_f(L) \approx 0.8E_f^{\text{RLD}}$ in agreement with measurements for lighter systems.

^(a)Also at Division of Mineral Physics, Commonwealth Scientific and Industrial Research Organization, North Ryde, 2113, N.S.W. Australia.

¹R. M. Diamond and F. S. Stephens, *Annu. Rev. Nucl.*

Sci. **30**, 85 (1980).

²M. Beckerman and M. Blann, *Phys. Rev. C* **17**, 1615 (1978), and references therein.

³F. Plasil *et al.*, *Phys. Rev. Lett.* **45**, 333 (1980).

⁴A. M. Zebelman *et al.*, *Phys. Rev. C* **10**, 200 (1974).

⁵D. J. Hinde *et al.*, to be published.

⁶R. G. Stokstad and E. E. Gross, *Phys. Rev. C* **23**, 281 (1981); K.-H. Möbius *et al.*, *Phys. Rev. Lett.* **46**, 1064 (1981).

⁷L. G. Moretto, *Nucl. Phys.* **A180**, 337 (1972).

⁸M. Beckerman and M. Blann, University of Rochester Report No. C00-3494-36 UR-NSRL-135, 1977 (unpublished).

⁹L. C. Vaz and J. M. Alexander, *Phys. Rev. C* **10**, 464 (1974).

¹⁰S. Cohen, F. Plasil, and W. J. Swiatecki, *Ann. Phys. (N.Y.)* **82**, 557 (1974).

¹¹R. Vandenbosch and J. R. Huizenga, *Nuclear Fission* (Academic, New York, 1973).

¹²J. R. Beene *et al.*, *Phys. Rev. C* **23**, 2463 (1981).

Third Discontinuity in the Yrast Levels of ^{158}Er

J. Burde,^(a) E. L. Dines,^(b) S. Shih,^(c) R. M. Diamond, J. E. Draper,^(b) K. H. Lindenberg,^(d)
C. Schück,^(e) and F. S. Stephens

Nuclear Science Division, Lawrence Berkeley Laboratory, University of California, Berkeley, California 94720

(Received 7 December 1981)

Discrete yrast transitions from states with spins up to $I=38$ have been observed in ^{158}Er via the reaction $^{122}\text{Sn}(^{40}\text{Ar}, 4n\gamma)$. In addition to the pronounced backbend at $I=14$ and the upbend at $I=28$ previously known, the start of a third yrast discontinuity at $I=38$ is indicated. Candidates for the $I=40$ state are suggested and possible causes of the yrast discontinuity are discussed.

PACS numbers: 21.10.Re, 23.20.Lv, 27.70.+q

In rare-earth nuclei states with angular momenta up to $I \approx 70$ can survive particle evaporation following heavy-ion fusion reactions.¹ However, the nuclear structure of states of very high angular momentum can be studied only through unresolved deexcitation γ rays.² Resolved γ lines from collective states have usually been observed only for $I < 30$, although for noncollective states spins as high as $I = 38$ have been identified.³ Many attempts have been made to extend these angular momentum limits because discrete γ rays can give more detailed nuclear structure information. The discovery⁴ of "backbending," where the regular frequency increase with spin is temporarily reversed, produced many investigations of collective states by (HI, xn) reactions and by Coulomb excitation. The explanation usually given for this discontinuity in the yrast levels is

the alignment of the angular momentum of two high- j nucleons with the rotational angular momentum.⁵ In ^{158}Er the backbend at $I = 14$ has been attributed to the alignment of a pair of $i_{13/2}$ neutrons,^{6,7} and the upbend at $I = 28$ has been considered as due most probably to alignment of a pair of $h_{11/2}$ protons.⁸ The aim of the present investigation was to study still higher members of the yrast sequence.

The high-spin yrast levels in ^{158}Er have been produced in the reaction $^{122}\text{Sn}(^{40}\text{Ar}, 4n)$ with use of 170-MeV ^{40}Ar projectiles from the 88-in. cyclotron of the Lawrence Berkeley Laboratory. The lifetimes of the states with spins $\geq 20\hbar$ observed in the present experiment are expected to be comparable to the stopping time of the excited recoiling nuclei in the target. Hence, with a thick target, 1-MeV γ lines will have a width